

Masses of ^{61}Fe and ^{62}Fe †

J. D. Cossairt, R. E. Tribble,* and R. A. Kenefick

Cyclotron Institute, Texas A & M University, College Station, Texas 77843

(Received 4 October 1976)

The mass excesses of ^{61}Fe and ^{62}Fe have been measured using the $^{64}\text{Ni}(\alpha, ^7\text{Be})^{61}\text{Fe}$ and $^{64}\text{Ni}(^{11}\text{B}, ^{13}\text{N})^{62}\text{Fe}$ reactions. The mass excesses obtained are $M(^{61}\text{Fe}) = -58.92 \pm 0.02$ MeV and $M(^{62}\text{Fe}) = -58.85 \pm 0.07$ MeV. The results are consistent with recent predictions from two different mass relations.

[NUCLEAR REACTIONS $^{64}\text{Ni}(\alpha, ^7\text{Be})$ and $^{64}\text{Ni}(^{11}\text{B}, ^{13}\text{N})$. Measured ^{61}Fe and ^{62}Fe masses. Compared with predictions.]

I. INTRODUCTION

In recent years a considerable effort has been invested by various workers in the development of accurate predictions of unknown nuclear masses. A general review of such nuclear mass relations has been given by Garvey.¹ In medium-mass nuclei, difference equations have been developed which use the known nuclear masses in an independent-particle model framework to predict those of neighboring nuclei. The predictions have been tabulated and where possible compared to known masses resulting in an rms deviation of 158 keV.² A slightly different approach, taking more explicit account of shell effects, has been developed by Jelley *et al.*³ Recently, Davids has extended the method of Ref. 3 to the mass region near iron,⁴ and reports an rms deviation from the known masses of 155 keV. It is important to test such predictions of neutron-rich nuclei, for it would be desirable to extend the predictions in an accurate manner to extremely neutron-rich nuclei. Such masses are important in understanding γ -process nucleosynthesis because of binding energy considerations.^{4,5} Mass measurements of the neutron-rich nuclei ^{61}Fe and ^{62}Fe provide useful tests of these predictions. Previously both masses have been deduced from their β decay.^{6,7} In the present work, Q -value determinations were employed to obtain more accurate mass measurements. Simultaneously spectra for low-lying excited states were obtained, thus providing the first spectroscopic information about ^{61}Fe and a determination of an unreported excited state in ^{62}Fe . During the course of this work, a different Q -value determination of the ^{62}Fe mass was reported by Hickey *et al.*⁸ In Sec. III, the present results are compared with the previous β decay and Q -value mass determinations, and with mass formula predictions. This work is a part of a larger effort at this laboratory concerned with the precise measurement

of nuclear mass excesses, some results of which have been discussed elsewhere.^{9,10}

II. EXPERIMENTAL PROCEDURE

The masses of the two nuclei of interest were measured using the $^{64}\text{Ni}(\alpha, ^7\text{Be})^{61}\text{Fe}$ reaction at 116.5 MeV and the $^{64}\text{Ni}(^{11}\text{B}, ^{13}\text{N})^{62}\text{Fe}$ reaction at 91 MeV with beams from the Texas A&M University 88-in. cyclotron. Reaction products were detected in the focal plane of an Enge split-pole magnetic spectrograph using a 10-cm resistive division single-wire proportional counter backed by a 5 cm \times 1 cm \times 500 μm Si solid-state detector. Particles were identified using the three constraints: (1) $(dE/dx)_{\text{gas}}$, (2) total energy, and (3) time of flight relative to the cyclotron rf. In all cases a gas consisting of 90% argon and 10% methane was continuously flowed through the gas counter. For the $(\alpha, ^7\text{Be})$ experiment the gas was maintained at 1 atm pressure and 12.7- μm thick Kapton entrance and exit windows were used on the gas counter. For the heavier ions encountered in the $(^{11}\text{B}, ^{13}\text{N})$ experiment the gas pressure was 0.33 atm and the windows were 6.4- μm aluminized Mylar. The spectrograph solid angle was 2.3 msr in both cases. Figures 1 and 2 are isometric plots showing samples of the particle identification capabilities of the detection system.

Calibration of the spectrograph focal plane was performed using the reaction involved in a given mass measurement on targets where all four nuclei involved have accurately known mass excesses. In all cases such calibration reactions involved only small (less than 2.4%) changes in the spectrograph magnetic field and calibration spectra were taken at several field settings bracketing the one used for the ^{64}Ni target.

In the case of the ^{61}Fe measurement, the $^{32}\text{S}(\alpha, ^7\text{Be})^{29}\text{Si}$ reaction using both the ground state and the 2.028-MeV state in ^{29}Si was used for the calibration. Preliminary runs with the same

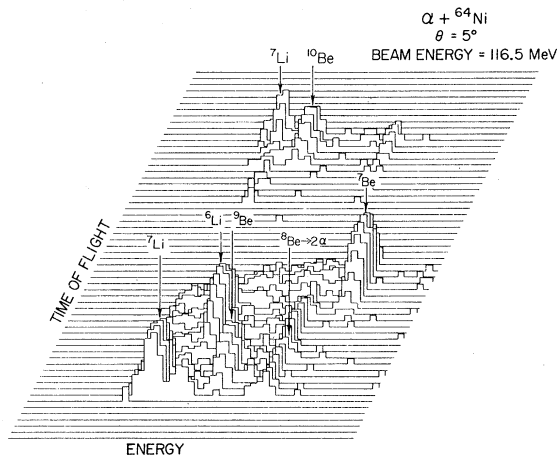


FIG. 1. Isometric plot of counts vs time of flight and total energy showing various particle groups produced by 116.5-MeV α particles on ^{64}Ni at 5° . The α groups from the breakup of ^8Be are also indicated.

reaction involving targets of ^{12}C , ^{24}Mg , and ^{16}O were used to verify the particle identification procedure and to check for possible contaminant peaks in the spectrum taken with the ^{64}Ni target. Runs were taken on some of these targets and on the ^{64}Ni target at both 5° and 10° laboratory scattering angles in order to help identify contaminant peaks by means of their kinematic shifts. No states due to such contaminants were seen in the ^{64}Ni spectra. The actual calibration runs with the sulfur target and the mass measurement run with the ^{64}Ni target were taken at 5° . A typical spectrum taken with the sulfur target is shown

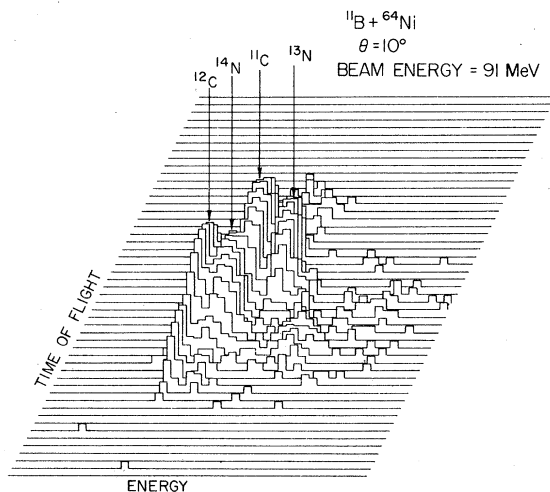


FIG. 2. Isometric plot of counts vs time of flight and total energy for the case of 91-MeV ^{11}B incident on ^{64}Ni at 10° .

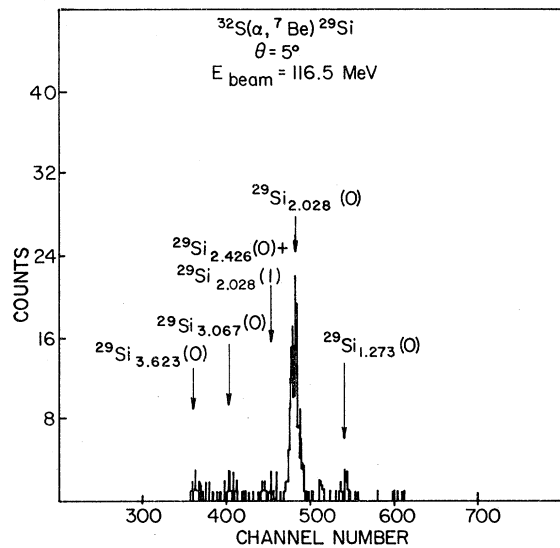


FIG. 3. $^{32}\text{S}(\alpha, ^7\text{Be})^{29}\text{Si}$ calibration spectrum at 5° lab. States are denoted thus: $^{29}\text{Si}(0)$ for $^{29}\text{Si} + ^7\text{Be}(g.s.)$ and $^{29}\text{Si}(L)$ for $^{29}\text{Si} + ^7\text{Be}(0.429)$.

in Fig. 3. The sulfur target was in the form of CdS 383 ± 38 - $\mu\text{g}/\text{cm}^2$ thick while the ^{64}Ni was in the form of a 436 ± 30 - $\mu\text{g}/\text{cm}^2$ rolled foil (enriched to 98% ^{64}Ni).

In the case of the ^{62}Fe measurement the $^{24}\text{Mg}(^{11}\text{B}, ^{13}\text{N})^{22}\text{Ne}$ reaction using both the ground and first-excited states of ^{22}Ne was the calibrant. A 283 ± 28 - $\mu\text{g}/\text{cm}^2$ ^{24}Mg target was used in this case. As in the ^{61}Fe measurement, other targets were also checked. In this case the calibration target and the ^{64}Ni target were bombarded at both 5° and 10° because of the possible presence of the ground-state peak from the $^{16}\text{O}(^{11}\text{B}, ^{13}\text{N})^{14}\text{C}$ reaction. Figure 4 shows a typical spectrum taken with the ^{24}Mg target. Figures 5, 6, and 7 show the spectra from the reactions involving the ^{64}Ni target. These spectra are plotted as a function of reaction Q value as determined by the calibration procedure.

In such precision mass measurements the determination of uncertainties is of crucial importance. Table I lists the contributions of various uncertainties to the total uncertainty in the measured masses. The uncertainty in the beam energy is a reflection of the calibration accuracy of the analyzing magnet NMR readout for the particular beams involved. Target thicknesses were measured using an ^{241}Am α source and where possible by weighing. The scattering angle was determined optically to an accuracy of $\pm 0.1^\circ$. Mass excesses and uncertainties for standard masses are those of Wapstra and Gove.¹¹ Including the uncertainties from Table I, the present results

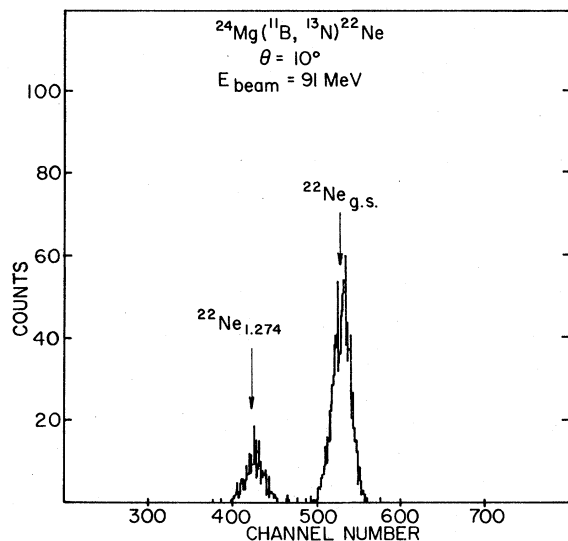


FIG. 4. $^{24}\text{Mg}(^{11}\text{B}, ^{13}\text{N})^{22}\text{Ne}$ calibration spectrum at 10° lab.

for the mass excesses are displayed in Table II along with previous β -decay and Q -value measurements.

III. RESULTS AND DISCUSSION

Figures 5, 6, and 7 show the spectra from the ^{64}Ni target. In the case of the $^{64}\text{Ni}(\alpha, ^7\text{Be})^{61}\text{Fe}$ reaction (Fig. 5) the position of the ^{13}C ground

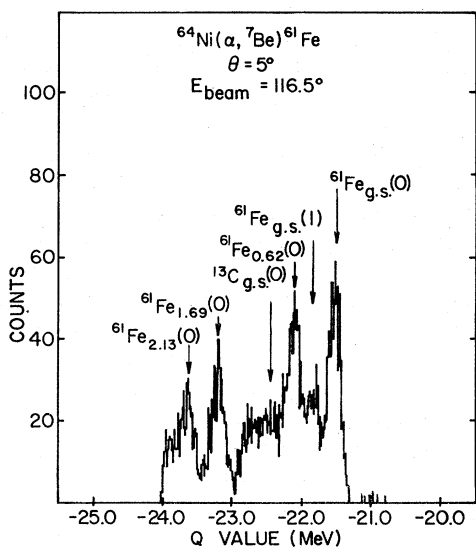


FIG. 5. $^{64}\text{Ni}(\alpha, ^7\text{Be})^{61}\text{Fe}$ position spectrum at 5° showing the low-lying states in ^{61}Fe and the position of a possible peak due to contaminant ^{16}O on the target. States are denoted thus: $^{61}\text{Fe}(0)$ for $^{61}\text{Fe} + ^7\text{Be}(\text{g.s.})$ and $^{61}\text{Fe}(1)$ for $^{61}\text{Fe} + ^7\text{Be}(0.429)$.

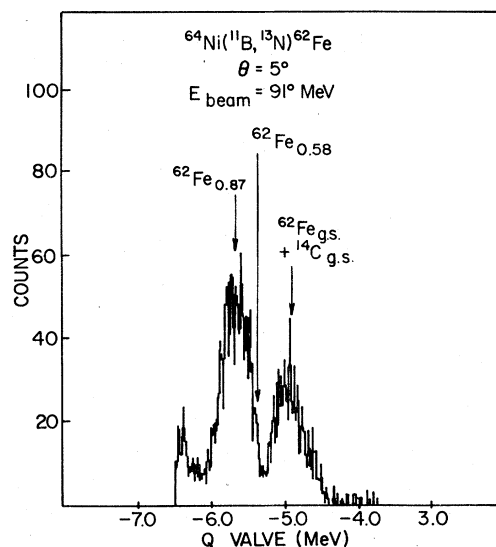


FIG. 6. $^{64}\text{Ni}(^{11}\text{B}, ^{13}\text{N})^{62}\text{Fe}$ position spectrum at 5° showing the lowest states in ^{62}Fe along with the expected position of a contaminant peak due to ^{16}O .

state due to possible ^{16}O contamination on the target is indicated. Also, it should be mentioned that both in other work involving the $(\alpha, ^7\text{Be})$ reaction and in the calibration spectra of the present experiment, significant population of the 0.429-MeV state in ^7Be is seen in some cases. However, it is generally populated considerably less strongly than is the ^7Be ground state.¹² The resolution in the present experiment was sufficient to cleanly resolve these two states. For

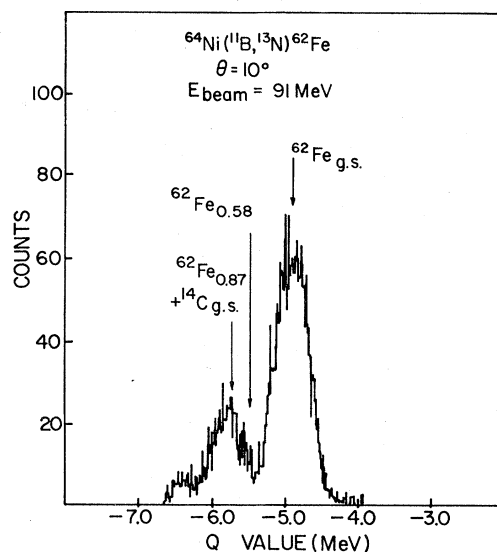


FIG. 7. $^{64}\text{Ni}(^{11}\text{B}, ^{13}\text{N})^{62}\text{Fe}$ position spectrum at 10° showing same states as Fig. 6.

TABLE I. Contributions to the uncertainties in the mass determinations (keV). Actual values are included in parentheses where required.

Variable	^{61}Fe	^{62}Fe
Beam energy	5.2 (116.5 \pm 0.2 MeV)	12.5 (91.0 \pm 0.5 MeV)
Focal plane calibration	11.2	5.3
Target thickness- ^{64}Ni	5.9	38.6
Calibrant	11.0	48.5
Centroid uncertainty	5.6	6.9
Uncertainty of masses	3.9	3.6
Scattering angle	2.8 (5.0 \pm 0.1) $^\circ$	10.0 (10.0 \pm 0.1) $^\circ$

example, in Fig. 5 the peak at $Q = -21.54$ is taken to be the ^{61}Fe ground state and ^7Be ground state, while the weaker state involving the ^{61}Fe g.s. and the ^7Be 0.429 state is also indicated. The spectrum indicates several excited states in the 2.5 MeV excitation range covered, a result which is not surprising for an odd- A nucleus. The excitation energies of the more strongly populated excited states of ^{61}Fe are indicated on Fig. 5. The uncertainties in their value are approximately ± 20 keV for the 0.62- and 1.09-MeV states. The uncertainty in the value for the 2.13-MeV state may be somewhat larger because of possible contamination from the $^{61}\text{Fe}_{1.69} + ^7\text{Be}_{0.429}$ state. The small number of counts at less negative Q values than the ^{61}Fe ground state probably result from the presence of other Ni isotopes in the target. It is improbable that these counts could be the $^{61}\text{Fe}(\text{g.s.}) + ^7\text{Be}(\text{g.s.})$, while the peak at $Q = -21.54$ MeV could be the $^{61}\text{Fe}(\text{g.s.}) + ^7\text{Be}(0.429)$ or an excited state in ^{61}Fe , because such a result would represent a disagreement of over four standard deviations with the previous experimental mass excess of -59.03 ± 0.07 MeV deduced from the β -decay work of Ref. 6. The counts in the assumed ground-state peak represent a differential cross section of about $6 \mu\text{b}/\text{sr}$. The position of this peak gives a mass excess for this nucleus of -58.92 ± 0.02 MeV. The present result is to be compared with the predictions -59.04 MeV from Ref. 2 and -58.53 MeV of Ref. 4. However, the calculations

of Ref. 4 are only for states of minimum seniority. Since the ground state of ^{61}Fe is not expected to be the state of minimum seniority, the mass excess of ^{61}Fe would be more negative than the prediction.

In Figs. 6 and 7 the population of the low-lying states of ^{62}Fe are shown at 5° and 10° . The ^{62}Fe spectrum is somewhat easier to interpret than the ^{61}Fe spectrum, since ^{13}N has no bound excited states. The measurement of the ground state Q value was performed at 10° because of the possible contributions from an oxygen contaminant near the ground state at 5° . Again, the counts at Q value less negative than the ground-state peak are probably due to other isotopes of Ni in the target. The yield to the ground-state peak represents a differential cross section of about $24 \mu\text{b}/\text{sr}$ at $\theta_{\text{lab}} = 10^\circ$. The mass excess is found to be -58.85 ± 0.07 MeV. Our result is not in good agreement with the β -decay measurement that determined the mass excess to be -58.5 ± 0.2 MeV (Ref. 7). We are in good agreement with the other Q -value determination which obtained a mass excess of -58.935 ± 0.050 MeV (Ref. 8). The authors of Ref. 8 report an excited state at $E_x = 580 \pm 50$ keV. In the present work we observe an excited state at $E_x = 870 \pm 20$ keV with possibly a weak indication of an additional state at 580 keV. The peak position corresponding to $E_x = 580$ keV is shown on the spectra obtained at both 5° and 10° . The present ^{62}Fe mass determination can be compared to the predicted values

TABLE II. Experimental mass determinations for ^{61}Fe and ^{62}Fe .

	Q value (MeV)	Present result	Mass excess (MeV)	
			β decay	Other Q-value determinations
^{61}Fe	-21.54 ± 0.02	-58.92 ± 0.02	-59.03 ± 0.07 (Ref. 10)	
^{62}Fe	-4.93 ± 0.07	-58.85 ± 0.07	-58.5 ± 0.2 (Ref. 12)	-58.935 ± 0.050^a (Ref. 11)

^a Q -value determination using the $^{64}\text{Ni}(^{18}\text{O}, ^{20}\text{Ne})^{62}\text{Fe}$ reaction.

of -59.41 MeV (Ref. 2) and -58.82 MeV (Ref. 4). The weighted average of the two Q -value determinations would tend to favor the result of Ref. 4.

It is of interest to use the two masses determined in the present work to check the accuracy of Eq. (1) of Ref. 2. Substituting $N=34$ and $Z=28$ (^{62}Ni) into this equation, one obtains the following:

$$^{62}\text{Fe} - ^{62}\text{Ni} + ^{61}\text{Co} - ^{61}\text{Fe} + ^{63}\text{Ni} - ^{63}\text{Co} = 0.$$

Substitution of the experimental mass excesses, including the present result for ^{61}Fe and a value of -58.906 ± 0.041 for ^{62}Fe (the weighted average of the present result and that of Ref. 8), gives a value of 179 ± 52 keV on the left-hand side. If the previous β -decay values for the mass excesses of ^{61}Fe and ^{62}Fe are used in Eq. (2), the left-hand side has a value of 0.7 ± 0.2 MeV, which is a significantly greater discrepancy. The same equation may also be used to predict the mass of ^{63}Fe since all the masses needed including ^{64}Co are now experimentally known.¹³ By taking (N, Z) to be $(35, 28)$ (^{63}Ni) one obtains a value of -55.60 ± 0.06 MeV compared with -56.12 MeV in Ref. 2 and -55.18 MeV in Ref. 4, a value which is again in between the tabulated values. If this mass excess is correct, ^{63}Fe would be stable to

decay by neutron emission by 4.8 MeV and to proton emission by about 14 MeV. A measurement of the mass of ^{63}Fe would thus provide a further test of the predictive power of the two procedures as the neutron number increases.

It would also be useful to have experimental values for the mass excesses of other neutron-rich nuclei in this mass region. As a part of this work an attempt was made to measure the mass of ^{60}Mn by means of the $^{64}\text{Ni}(\alpha, ^8\text{B})^{60}\text{Mn}$ reaction at 116.5 MeV. No definite transitions to ^{60}Mn were observed, corresponding to an upper limit cross section of 10 nb/sr in the Q -value window from -33 to -38 MeV. The value of the mass of ^{60}Mn tabulated in Ref. 1 would give a Q value of -34.66 MeV. Since the cross section appears to be small and ^{60}Mn is an odd-odd nucleus likely to have a complicated level scheme, further attempts have not been made. A brief attempt has also been made to measure the mass of ^{61}Mn by means of the $^{64}\text{Ni}(^{11}\text{B}, ^{14}\text{O})^{61}\text{Mn}$ reaction at 91 MeV with negative results similar to those obtained for ^{60}Mn .

The authors gratefully acknowledge the support of the cyclotron operations staff throughout the course of these measurements.

†Supported in part by the National Science Foundation.

*Alfred P. Sloan Fellow, 1976-1978.

¹G. T. Garvey, *Annu. Rev. Nucl. Sci.* **19**, 433 (1969).

²G. T. Garvey, W. J. Gerace, R. L. Jaffe, I. Talmi, and I. Kelson, *Rev. Mod. Phys.* **41**, S1 (1969).

³N. A. Jelley, J. Cerny, D. P. Stahel, and K. H. Wilcox, *Phys. Rev. C* **11**, 2049 (1975).

⁴C. N. Davids, *Phys. Rev. C* **13**, 887 (1976).

⁵D. D. Clayton, *Principles of Stellar Evolution and Nucleosynthesis* (McGraw-Hill, New York, 1968), p. 582.

⁶R. L. Auble, *Nucl. Data Sheets* **16**, 1 (1975).

⁷E.-M. Franz, S. Katcoff, H. A. Smith, Jr., and T. E. Ward, *Phys. Rev. C* **12**, 616 (1975).

⁸G. T. Hickey, G. M. Crawley, D. C. Weisser, and N. Shikazono, *J. Phys. G* **2**, L143 (1976).

⁹R. E. Tribble, R. A. Kenefick, and R. L. Spross, *Phys. Rev. C* **13**, 50 (1976).

¹⁰R. E. Tribble, J. D. Cossairt, and R. A. Kenefick, *Phys. Lett.* **61B**, 353 (1976).

¹¹A. H. Wapstra and N. B. Gove, *Nucl. Data A* **9**, 265 (1971).

¹²N. A. Jelley, K. H. Wilcox, R. B. Weisenmiller, G. J. Wozniak, and J. Cerny, *Phys. Rev. C* **9**, 2067 (1974).

¹³E. R. Flynn and J. D. Garrett, *Phys. Lett.* **42B**, 49 (1972).